View metadata, citation and similar papers at core.ac.uk
brought to you by CORE
provided by St George's Online Research Archive

Proof of Concept Study of a Novel Pacemapping Algorithm as a Basis to Guide Ablation of Ventricular Arrhythmias

Short Title: Li: Evaluation of a pacemapping navigation algorithm

Anthony Li[a], MBBS, MD; Joseph Samuel Davis[b], MS; Alexander Grimster[a], BSc; Jeremiah Wierwille[b], PhD; Keith Herold[b], PhD; Dennis Morgan[c], MS; Elijah Behr[a], MD; Stephen Shorofsky[d], MD, PhD, FHRS; Magdi Saba[a], MD, FHRS.

[a]Cardiology Clinical Academic Group, St. George's University of London, London, UK.
[b]Fischell Department of Bioengineering, Clark School of Engineering, University of Maryland, College Park, Maryland, USA.
[c]St. Jude Medical, St. Paul, Minnesota, USA.
[d]Division of Cardiology, Department of Medicine, University of Maryland Medical System, Baltimore, Maryland, USA.

Corresponding Author:
Dr Anthony Li
Cardiology Clinical Academic Group
St. George's University of London
Blackshaw road
London. U.K. SW17 0RE
Tel +44208 725 1390
Email: ali@sgul.ac.uk

Word count: 4,486

Journal Subject Terms: Arrhythmias, Catheter Ablation and Implantable Cardioverter-Defibrillator

Sources of Funding: This work was supported by a fellowship grant from St Jude Medical.

Disclosures: Dr Li received fellowship support from St Jude Medical. Mr Morgan is an employee of St Jude Medical. Drs Saba and Shorofsky received a moderate grant from St Jude Medical and have ownership of intellectual property pertaining to the mapping algorithm referred to in the manuscript. The other authors report no conflicts.

Abstract

Aims

To determine if a software algorithm can use an individualised distance-morphology difference model, built from 3 initial pacemaps, to prospectively locate the exit site (ES) of ventricular arrhythmias (VA).

Methods

Consecutive patients undergoing ablation of VA from a single centre were recruited. During mapping, 3 initial pacing points were collected in the chamber of interest and the navigation algorithm applied to predict the ES, which was corroborated by conventional mapping techniques.

Results

Thirty-two patients underwent ES prediction over 35 procedures. Structural heart disease was present in 16 (7 ICM, 9 NICM), median EF 45% (IQR 26). The remainder had normal hearts. The navigation algorithm was applied to 46 VA (24 LV, 11 RVOT, 5 LVOT, 4 RV, 2 epicardial) and successfully located the site of best pacemap match in 45 within a median area of 196.5mm^2 (IQR 161.3, range 46.6-1288.2mm^2).

Conclusions

In a diverse population of patients with and without structural heart disease, the ES of VA can be accurately and reliably identified to within a clinically useful target area using a simple software navigation algorithm based on pacemapping.

Keywords: Pacemapping; Ventricular tachycardia; Ventricular ectopy; Mapping

Condensed Abstract

A pacemapping software algorithm based on the construction of an individualised distance-morphology difference model was utilised in 32 patients with and without structural heart disease. The exit site of 45/46 ventricular arrhythmias was successfully triangulated to within an area of 197mm^2. The algorithm can be automated in future versions.

What's New?

- The exit site of ventricular arrhythmias can be successfully triangulated using a simple software algorithm based on pacemapping.
- The navigation algorithm can be successfully applied to an individualised distance-morphology difference model constructed from only 3 initial pacemaps.
- The algorithm can be used successfully in normal hearts and in the presence of structural heart disease.
- The navigation algorithm has the potential to become fully automated.

Introduction

Pacemapping is an established technique to locate the exit site (ES) of ventricular arrhythmias (VA). [1] Currently, there is no system that guides the physician to a location where a closer pacemap match could be obtained. We have previously reported that a robust relationship exists between the change in ECG morphology and the distance between pacing points when limiting pacing to areas of preserved myocardial voltage. [2] Using this relationship, it may be possible to estimate the distance between the ES of a VA and several pacing points, to predict the exit site.

This study aims to investigate whether the construction of an individualised distance-ECG morphology difference model could facilitate the identification of a VA ES in patients with and without structural heart disease using a novel pacemapping algorithm. This could form the basis of an automated navigation system which could reduce the burden on the operator.

Methods

Patient characteristics

The subjects of this study were 38 consecutive patients who underwent VA ablation procedures at St. George's Hospital between February 2013 and July 2014. The study was approved by the National Research Ethics Service and individual written informed consent was obtained. Cardiac etiology was established by conventional diagnostic criteria. All patients underwent transthoracic echocardiography or cardiac MRI and coronary angiography in cases of structural heart disease.

Procedural protocol

Our mapping protocol has been described previously. [2] All studies were performed on patients in the post-absorptive state, whose antiarrhythmic drug therapy was discontinued for at least 5 half-lives, except in patients on Amiodarone. Scar-dependent VT ablation was performed under general anesthesia and ventricular ectopy (VE) cases under light conscious sedation. The decision to perform epicardial access was based on the following: ECG features suggestive of an epicardial site,

unsuccessful endocardial ablation/mapping indicating an epicardial focus, epicardial scar on cardiac MRI (CMR) or substrate known to be associated with epicardial circuits.. ECG electrodes were placed in a standard configuration with surface ECG filter settings at 0.5-100Hz with a 50Hz notch filter enabled. Electro-anatomical mapping was performed using the Ensite Velocity System (St. Jude Medical, St Paul, MN, USA) and data simultaneously logged on Labsystem Pro software (Bard electrophysiology, Lowell, MA, USA) and bipolar electrograms recorded with filter settings at 30-300 Hz. Multipolar catheters were introduced into the coronary sinus and right ventricle in all cases. Mapping and ablation were performed with a 3.5mm open irrigated ThermoCool SF catheter (Biosense-Webster, Diamond Bar, CA, USA).

For VT cases, voltage mapping was performed during sinus rhythm, concentrating on areas of abnormal voltage, with a fill threshold of 10mm, using established definitions of scar (<0.5mV for dense and >1.5mV for normal tissue). For VE cases, voltage mapping was discretionary.

Navigation concept

Custom software was coded into a research platform of the Ensite Velocity system (St. Jude Medical, St Paul, MN, USA) that ran parallel to the commercial platform and utilised a data switch to run identical data streams from the amplifier to each system. A workflow for the navigation is shown in Figure 1 and Figure 2. Once voltage mapping was completed, an ECG template of the clinical VA was assigned as the target on the navigation platform. If there was no VE at baseline, intravenous isoprenaline infusion was used. In VT cases, induction with two drive cycle lengths and up to 3 extrastimuli was undertaken from multiple sites. If non-inducible, the patient was excluded from the study. After the clinical VA was captured, calipers were assigned to mark the QRS onset and offset to facilitate automatic alignment of subsequent pacemaps using the maximum of the 12-lead composite signal (maximum energy).

Pacing was performed at 2ms pulse width at just above threshold and at the coupling interval or cycle length of the clinical VA or, if haemodynamically unstable at that rate, at 400ms, during sinus

rhythm from the distal bipole of the mapping catheter. Pacing points were restricted to myocardium >0.5mV as displayed on the voltage map and were initially placed at 3 widely spaced sites within the chamber of interest, based on the VA morphology. In general, for RBBB pattern VA, the left ventricle was the chamber of interest and for LBBB pattern VA, the right ventricle. In cases with scar, the initial pacing sites were spaced equally to surround the scar. Pacing was initiated at low output and increased until ≥3 consecutive identical captured beats without evidence of fusion were obtained. The last identical beat was then selected and automatically aligned over the clinical VA. Figure 2A. If unsatisfactory alignment occurred, manual adjustments were allowed.

Once 3 pacing points were captured, the navigation algorithm is applied, which plots the Euclidean distances between pacing points against the difference in their morphology calculated by applying the root mean square sum metric across all 12-ECG leads (E12) as previously described.[2] This equation, in essence, quantifies the difference in the area under the curve for each QRS morphology in the 12-lead ECG within the window of interest. The value of E12 is zero for identical 12-lead ECG tracings and increasingly larger for data sets that have greater dissimilarity, thus providing a direct measure of the similarity between two ECG traces.

The E12 – a quantitative difference in ECG morphology - is then plotted against the Euclidean distance between pacing points. Origin-constrained least squares linear regression of the E12-distance plot is then calculated to produce a slope which represents the patient specific distance-E12 model (DEM). Figure 2B. The E12 morphology difference between the clinical VA and each pacing point is then calculated and plotted along the DEM which results in estimated distances that the clinical VA should lie from each pacing point. Figure 2C. The estimated distances are then used as the radii of spheres which are displayed on the geometry surface as overlapping circles. The area where all 3 circles overlap should contain the ES of the clinical VA (Figure 2D). Offsetting the regression line rightward (larger estimated distance per E12), to a degree proportionate to the amount of variance in the model, ensured that the radii are large enough to reliably encompass the ES of the clinical VA.

For weaker models with a large variance, adjusting the required rightward offset will result in a larger increase in estimated distance compared with stronger models with smaller variance.

If the estimated distances - and thus the target area - is large, the pacing site with the furthest estimated distance from the clinical VA is replaced with an additional pacing site that is nearer to or within the target area, the location of which is guided by the position and estimated distances from the other pacing sites. Optimally, the additional pacing site is selected such that the new combination of pacing sites surrounds the suggested target area. This process was repeated iteratively until the target area was minimised. Figures 3 and 4. Each pacing site that is collected can be assigned to contribute to the DEM, which is recalculated each time, or for target visualisation, or both. If a pacing site had an estimated distance of >50mm from the target or from other pacing sites, this was removed from the DEM as our prior data had shown that the association between change in E12 per unit distance becomes non-significant at greater distances.[2]

Although the operator could map the VA in real-time with the software, it was not intended that it was to be used as the sole mapping method to guide ablation. As such, conventional methods were used to confirm the accuracy of the algorithm. In all VE cases, activation mapping was used to define the ES. In cases of haemodynamically stable VT, entrainment and limited activation mapping were performed to identify the isthmus and its associated ES. Where VT was unstable, pacemapping at borderzone areas and at sites of local abnormal activity was performed to identify the exit.[3] For the purposes of analysis, an area of excellent (≥ 11/12) pacemap match with S-QRS < 40ms at the borderzone was taken to be the ES for the VA and was targeted for ablation along with abolition of associated abnormal local electrical activity.

Outcome

The end-point of efficacy of the algorithm was the frequency of attainment of the best possible pace-map match (least possible E12) to the clinical VA within the smallest achievable target surface area predicted by the navigation algorithm.

Patients were routinely followed up and assessed at clinic visits with repeat Holter monitoring or device interrogations where applicable.

Statistical Analysis

Statistical analysis was carried out with R version 2.15.2 (R Foundation for Statistical Computing, Vienna, Austria) and STATA version 13.0 (StataCorp, College Station, Texas, USA). The distribution of continuous variables was assessed for normality using the Shapiro-Wilk test. Comparisons between groups of continuous data were carried out by t-test after controlling for equality of variance with Levene's test. Non-normal distributed variables were analysed with Mann-Whitney U test and categorical data were compared with the Chi-square test. Univariable and multivariable linear mixed-effects models with random intercept and unstructured covariance matrix were used to investigate the effect of variables on target size. Variables found to be significantly associated with target size in univariable analysis were entered into the multivariable model. Statistical significance was set at <0.05.

Results

Patient demographics and procedural characteristics

Patient demographics are summarised in Table 1. Thirty-eight patients were enrolled in the study. Six were excluded due to non-inducibility. Thirty-two patients underwent real-time ES prediction using the navigation software in 35 separate procedures. One patient underwent 3 procedures and another, 2. Equal numbers of patients were recruited to the normal and structural heart disease groups. Ischaemic cardiomyopathy was the predominant aetiology of structural heart disease (44%) followed by idiopathic dilated cardiomyopathy (19%).

Procedural characteristics are shown in Table 2. Sixteen procedures were undertaken in structurally normal hearts. Ablation was predominantly for VE (81%) in normal hearts and for VT (68%) in cases of structural heart disease.

Mapping

Mapping data are presented in Table 3. Forty-six VAs underwent real-time ES prediction, of which 18 (39%) were in normal hearts. The predominant ES was the RVOT (56%) in normal hearts and the LV (79%) in structural heart disease patients. A median of 5 (IQR 2) pacing points were used to construct the DEM overall with no difference between cardiac aetiologies. Correlation between distance and E12 points for each DEM were high, with a median R^2 of 0.96. There was no significant difference between normal heart and structural heart disease cases in DEM R^2 values (0.96; IQR 0.09 vs. 0.95; IQR 0.05 p=0.737), variance of the DEM (3.92 SD 2.38 vs. 3.67 SD 2.10, p=0.86), nor slope of the DEM (0.26 SD 0.11 vs. 0.27 SD 0.12; p=0.64).

Accuracy of the navigation algorithm

The algorithm successfully navigated to an area containing the best pacemap match for 45/46 (98%) VAs. In two cases, the target was internal to the surface geometry. In both cases, the algorithm correctly arrived at the best pacemap site, but due to the small predicted distances and their location, internal to the geometry, the area of overlap of the spheres was not adequately projected onto the surface. One VA was mapped to the anterolateral LV papillary muscle and the other to the aortomitral continuity. The visible target area had an overall median area of 196.5mm^2 (IQR 161.3, range 46.6-1288.2mm^2). Mean E12 to the clinical VA at the target site was 2.77mV SD 1.25. The mean distance between first 3 pacemaps in the first iteration of the algorithm was 64.4mm SD 34.5 compared to the final iteration using 3 pacemaps for target prediction of 15.3 mm SD 10.

When comparing non-scar versus scar aetiologies, there was no significant difference in median target area, 208.9mm^2 (IQR 126.6) vs. 187.4mm^2 (IQR 180.3) p=0.804, respectively.

When analysing the target area by location, median areas were 228.2mm^2 (IQR 102.7) for 11 RVOT VAs, 253.6mm^2 (IQR 209.5) for 22 LV VAs, 120mm^2 (IQR 89.5) for 4 LVOT VAs, 186.3mm^2 (IQR 311.8) for 4 RV VAs and 139.2mm^2 for 2 epicardial LV VAs. Although no statistically significant differences were found when comparing target size by location, there were small numbers in each subset.

In multivariable analysis, neither presence of, or type of structural heart disease, nor LVEF, were predictors of target size. Furthermore, no significant association was found between the number of pacing sites used, correlation values, slope or variance of the DEM and target area achieved. Only the estimated distance, derived from the DEM, from each of the pacing sites used to predict the ES of the clinical VA was positively associated with target size (20.78mm^2 per mm distance, 95% CI 0.35, 41.22).

In one case, the algorithm failed to identify a suitable target. In this instance, limited substrate mapping was performed and retrospective analysis of the pacing sites demonstrated significant pacing latency within local bipolar voltage < 0.5mV that represented distant breakout from within scar.

Multiple VA mapping

In 9 procedures, ≥1 VA were mapped (20 VA in total, mean 2.2 per procedure). Eight of these were in scar-based aetiologies which had 17 VTs exiting from the LV, 2 of which had epicardial exits. In this group, 1 patient had 3 LV VTs mapped in the same procedure. In the remaining procedure, 3 VEs were mapped and ablated in a structurally normal heart from the RVOT, RV and LV.

Pairwise analysis of the data for scar-based LV exits showed that there was no significant difference when comparing the final map of the first VT compared to the last VT either in number of pacing sites used for the final DEM (p=0.67), target size (p=0.59), correlation values (p=0.68), slope of the DEM (p=0.68), or variance in the model (p=0.26).

When comparing the number of pacing sites used for the first and last VA prediction, pacing sites from the first prediction were utilised for the subsequent prediction in 5 cases, all within the same chamber, with a mean of 2.2 (range 1-3) pacing sites being reused.

Epicardial mapping

Three patients underwent combined endocardial-epicardial approach. All patients were male, median age 68 years (range 40-77) and had NICM with a median LVEF of 48% (range 23-55). Only one patient had a previous failed endocardial ablation. A total of 4 VT morphologies (2 epicardial exits) were mapped with the algorithm. The DEMs were constructed and target prediction performed using a combination of endocardial and epicardial pacing sites, (median 5 (range 4-7)). Mean distance between pacing sites was 21.3mm (range 6.9-41.7). Mean E12 between pacing sites was 4.6mV (range 1.6-10.0). Correlation values for the DEM were high; mean R^2=0.96. Using the algorithm, median target area containing the best pacemap match was 264mm^2 (range 115-732mm^2). In 2 instances (1 epicardial), the target area only projected onto a single surface, the diameter of the target area being shorter than the distance between epicardial and endocardial surfaces (Figure 5).

Acute procedure outcomes

Acute procedure success, defined by elimination of the clinically targeted VA, was achieved in 34/35 (97%). One RV papillary muscle VE was repeatedly supressed but not eliminated. If guided by the algorithm alone, the successful ablation lesion set lay within the target area in 43 (94%), within an immediately adjacent area in 2 (4%) and in 1 (2%), a target was not produced.

Long term follow up

Patients were followed up for a median of 567 days (IQR 989). Of the VE ablations, 3/16 patients had a recurrence of the clinical VE. In 2 patients with VE recurrences (1 with 3 ablations during the study period), an LV papillary muscle and RV papillary muscle VE was targeted initially and both are awaiting bipolar ablation. In the other patient with recurrence, a further trigger ablation for

Catecholaminergic Polymorphic VT was not attempted, and the patient underwent cervical sympathetic ganglionectomy with subsequent successful control of arrhythmia. For the remainder, VE ablation resulted in a reduction in burden of 14% IQR 12 to 0.3% IQR 1 at follow up.

2/16 patients who underwent VT ablation had recurrences during follow-up. In one, a single slow VT was targeted endocardially in a patient with ICM with multiple VT morphologies targeted at first attempt. The other required an epicardial procedure targeting de novo VT morphologies after a prior endocardial only procedure for subsequently diagnosed ARVC.

Discussion

The main findings of this study are that an individualised distance-E12 model can be constructed from 3 initial pacing points. This model can be exploited, using a simple software algorithm, to reliably locate the ES of a VA within a clinically useful target area.

The algorithm successfully predicted the site of best pacemap match in 45/46 VA within a median area of 197mm^2. This is equivalent to a circular area of radius 7.9mm or approximately the size of a 1 Cent Euro coin. A median of 5 pacing sites (including the initial 3) were used to rapidly construct the DEM and identify the target area. Although some targets had relatively large areas, integration with the voltage map in scar-related VT meant that further efforts were focused at the border zone harbouring the ES (Figure 3).

The single instance where the algorithm failed to identify a target was due to pacing at sites without sufficient delineation of substrate in that area leading to inadvertent pacing within scar and latency resulting in similar QRS morphologies being produced from catheter tip positions that were distant from each other. Therefore, it is still possible for the operator to be misled based on voltage map appearances due to colour interpolation and fill threshold. This could be addressed using conditional/logical operators in an automated program that serve to screen the quality of the pacing points against pre-defined criteria. Similarly, avoiding specialised conduction tissue may ensure that

the QRS morphology is representative of local myocardial capture. Discordance between the site of successful ablation and the area of best pacemap match is a known caveat of pacemapping and as such, this navigation algorithm would be similarly affected. In two instances, the target area was displayed in an adjacent area in close proximity to the ablation site and would still be expected to provide complimentary information to guide additional mapping efforts.

Multiple ES prediction was performed successfully in 9 procedures, which were mostly performed in the LV. Due to the design of the study it was not possible to detect any differences in the time taken to locate the ES between 1st, 2nd and 3rd prediction. However, the re-use of pacing sites for the DEM in 5/9 cases suggests that performing a second ES prediction within the same chamber is likely to require less time.

Experience of using the navigation algorithm in combined endocardial/epicardial procedures was limited to only 3 cases in the left ventricle. Of interest was that a combination of pacing sites on both surfaces in close proximity to each other appeared to produce a DEM of sufficient gradient to limit the target to one surface in 2 cases. In its current state, it is not expected to be able to predict an epicardial from an endocardial ES using only endocardial pacing sites. However, the lack of an adequate match or attainment of an excessively large target area, in conjunction with other electrocardiographic features, a future refined system could be programmed to suggest an alternative approach to the user. As the navigation concept provides an individualised model for each patient, it is conceivable that in a future iteration of the software, an epicardial site of origin could be predicted based on parameters such as the increase in maximal deflection index. Whereas current ECG algorithms use absolute values to predict an epicardial site of origin, this may be influenced by scar or antiarrhythmic use across individuals. A limited number of pacemapping studies have reported various surface ECG morphology indices to predict an epicardial origin of VT. [5] Furthermore, one study reported that a computerised learning algorithm could reliably discern epicardial from endocardial pacemaps in 80% of cases across chambers in normal hearts, ICM and

NICM.[6] Taken together, these data suggest that the ECG morphology produced by pacing either side of the ventricular wall is sufficiently different to be discerned by quantitative means.

Comparison to other pacemapping algorithms

The only other software-based pacemapping navigation in clinical use is the PASO™ module available for the CARTO platform (Biosense-Webster, Diamond Bar, CA, USA). This software uses the correlation coefficient to compare pacemaps to the clinical VA and uses a simple colour display to provide a visual reference to the correlation value. [7]

The major difference between this and our algorithm is that once a pacemap has been taken, the operator has no guidance as to where to move next to achieve a closer match. Our algorithm is able to provide both directionality and distance estimation to a next suitable site after considering the relative position of the pacing sites. Although ECG algorithms exist to predict the ES of VA and experienced operators may be able to mentally process ECG vectors, differences in patient anatomy and lead placement are limitations to these approaches. Therefore, constructing an individualised DEM, using the patient as their own "control", may provide incremental benefit. In this early version of the software, the operator must integrate the visual display with the distance data to identify the next site to pace to achieve a smaller target area. However, it is expected that in future iterations of this system this process could be fully automated.

Algorithm Functionality

The navigation concept provides a computationally simple algorithm using pacemapping and as such, will possess the same caveats as traditional pacemapping. We have previously shown that the DEM is robust between patients and in the presence and absence of structural heart disease.[2] However, navigation based on pacemapping may be problematic in areas where abrupt changes in QRS morphology could occur over short distances such as across the inter-ventricular septum, the aortic root or in areas containing Purkinje fibres where fusion of local myocardial and conduction tissue capture may occur and differences in morphology may be produced by altering pacing output.

Similarly, pacemapping within dense scar with latency may indicate a breakout at a distance from the catheter tip position and would therefore be expected to mislead the algorithm

When constructing the individual DEM for ES prediction, the algorithm forces the intercept of the model through the origin such that at distance = 0, E12 = 0. Therefore, the target area will contain a site of best pacemap match, but this does not necessarily equate to an area encompassing all possible best pacemap sites. When choosing the initial 3 sites to build the DEM and perform the first iteration of guidance, the greatest guidance for the initial step is expected to be optimal where the initial pacemaps are more morphologically distinct and therefore widely spaced. Should the operator choose a close grouping for the initial prediction, as long as the ECG morphology between pacemap points can be discerned with the E12 parameter, the algorithm is expected to still guide the user to perform further pacemapping at an alternative site with a closer match. However, the number of iterations required to minimize the target area would be larger.

The algorithm utilises the direct Euclidian distances as calculated from the Cartesian coordinates of the catheter tip. Prior analysis using geodesic distances, calculated by a recursive algorithm of the Euclidian distances between surface cloud points (unpublished), demonstrated no difference in the DEM at distances <50mm. Any difference between the two methods of distance measurement is likely to be clinically insignificant at shorter distances.

Although no statistically significant difference was found when comparing target size by location, the low number of VAs in certain locations precludes drawing firm conclusions.

Limiting pacing sites to areas of preserved voltage may also become problematic in patients with multiple territory scarring with regards to positioning of the 3 initial pacing sites to surround scar.

Despite these limitations we have shown, in this proof of concept study, that a software-based navigation algorithm using data from the 12-lead ECG and the 3D mapping system, without the need for any additional equipment, could form the basis of an automated or expert guidance system - a

rule-based system that can emulate the decision-making of a human expert. The advantage of the software lies in its simplicity, such that it can be coded into any current 3D mapping system. It is expected that further refinements will improve on its accuracy and reduce the target size. However, the algorithm is not envisaged to be used as a sole means of navigation and would provide complimentary data as part of an automated software package. In this respect, its main use would be to allow the operator to rapidly home in on a small target region of interest in order to further refine the area with high density activation mapping or refinement by high density pacemapping.

Study limitations

As discussed in previous sections, the navigation algorithm is based on pacemapping and therefore suffers from the same inherent limitations such as pacemapping within scar or where abrupt changes in morphology at short distances occur such as the septum.

Pacing in bipolar mode and with a 3.5 mm tip catheter may have resulted in capture of a larger area of myocardium than during unipolar pacing or pacing from catheters with small size electrodes.

During the real-time mapping studies, both operators could view the morphology of the clinical VA. This is the information conventionally available to operators and although regionalising to a chamber of interest does require some experience, any introduced bias would be minimal as the guidance system is not intended to be used in a blinded fashion. We therefore did not prospectively apply the algorithm to the opposite chamber to that of the clinical VA such as in the case of mapping the RV in a right bundle branch block morphology tachycardia. Retrospective analysis of an LV VT utilising the algorithm on either side of the interventricular septum demonstrates algorithm performance as shown in supplemental figure 1. None of the cases had an intra-septal VT focus and LV septal VTs were reliably discerned by their bundle branch morphology and so the requirement to map the RV septum and use the algorithm in a blinded fashion was not performed. Similarly, the algorithm was not tested across the RVOT/LVOT septum. In the few cases of LVOT VE, the morphology of the clinical beat had a RBBB or atypical RBBB morphology in V1 and therefore RVOT mapping was not

undertaken. Conversely, in LBBB VE, the RVOT was mapped first and if the algorithm, backed up by conventional mapping, confirmed an RVOT exit then ablation was applied and if suppression achieved then the Aorta was not accessed. Therefore, it is unknown how the algorithm would function across the outflow tract septum.

Conclusions

This study shows that an individualised distance-E12 model constructed from 3 initial pacing sites can form the basis of a computationally simple navigation algorithm that can reliably identify the ES of a VA to within a clinically useful target area. This provides the basis of an automated system that may expedite VA ablation procedures and reduce the burden on the physician.

Acknowledgements

Statistical support was provided by Mr Emmanouil Bagkeris at University College London.

References

1. Josephson ME, Waxman HL, Cain ME, Gardner MJ, Buxton AE. Ventricular activation during ventricular endocardial pacing. II. Role of pace-mapping to localize origin of ventricular tachycardia. *Am J Cardiol* 1982;**50**:11–22.

2. Li A, Davis JS, Wierwille J, Herold K, Morgan D, Behr E, *et al.* Relationship Between Distance and Change in Surface ECG Morphology During Pacemapping as a Guide to Ablation of Ventricular Arrhythmias. *Circ Arrhythmia Electrophysiol* 2017;**10**:e004447.

3. Nayyar S, Wilson L, Ganesan AN, Sullivan T, Kuklik P, Chapman D, *et al.* High-density mapping of ventricular scar: a comparison of ventricular tachycardia (VT) supporting channels with channels that do not support VT. *Circ Arrhythm Electrophysiol* 2014;**7**:90–8.

4. Moreno J, Quintanilla JG, Molina-Morúa R, García-Torrent MJ, Angulo-Hernández MJ, Curiel-Llamazares C, *et al.* Morphological and thermodynamic comparison of the lesions created by 4 open-irrigated catheters in 2 experimental models. *J Cardiovasc Electrophysiol* 2014;**25**:1391–9.

5. Berruezo A, Mont L, Nava S, Chueca E, Bartholomay E, Brugada J. Electrocardiographic recognition of the epicardial origin of ventricular tachycardias. *Circulation* 2004;**109**:1842–7.

6. Yokokawa M, Jung DY, Joseph KK, Hero AO, Morady F, Bogun F. Computerized analysis of the 12-lead electrocardiogram to identify epicardial ventricular tachycardia exit sites. *Heart Rhythm* 2014;**11**:1966–73.

7. Chang Y-T, Lin Y-J, Chung F-P, Lo L-W, Hu Y-F, Chang S-L, *et al.* Ablation of ventricular arrhythmia originating at the papillary muscle using an automatic pacemapping module. *Heart Rhythm* 2016;**13**:1431–40.

Figure Legends

Figure 1: Navigation algorithm workflow. DEM, distance-E12 model, VA, ventricular arrhythmia.

Figure 2: Navigation algorithm function. Please see text for detailed explanation. Panel A: Automatic alignment and calculation of E12 using the root mean square error metric between 2 ECG signals (purple and white) Panel B: An individual distance-E12 model is constructed with 3 pacing points (blue diamonds). R1-3 represents the estimated distances from each pacing point that a clinical VA resides based on the difference in E12. Panel C: R1-3 distances from each pacing site (green dots) form the radii of 3 overlapping circles. Blue indicates no overlap, yellow, overlap of 2 circles, red target area containing the arrhythmia exit (pink dot). Panel D: Target area overlaid onto the 3D surface geometry. AP = antero-posterior.

Figure 3: Normal heart VE from the RV free wall. Top left: Three initial widely spaced pacing points are used to produce an initial exit site prediction. Bottom left: Point 3 is substituted with an additional pacing point 4, taken nearer the target area resulting in a target area of 138.5mm^2. Middle panel: The ECG morphology of the clinical ectopic. Right panel: Activation map showing the earliest site of activation (red) and the successful lesion set (brown dots).

Figure 4: Ischemic VT exiting from the LV endocardium. Left panels: Inferior view of the LV showing 3 iterative steps with successive substitution of pacing points to achieve a smallest target area of 347mm^2 (red). Middle panel: ECG morphology of the clinical VT. Right panel: Electro-anatomical voltage map of the LV with successful ablation lesion set. Arrow indicates critical isthmus where ablation terminated the tachycardia. ECF, entrainment with concealed fusion.

Figure 5: Non-ischemic VT exiting from the LV epicardium. Left panel: ECG morphology of the clinical VT. Top right panel: Prediction of the site of successful ablation (red) of an epicardial focus using pacing points gathered from endocardial and epicardial surfaces to construct the distance-E12

model. Bottom right: Endocardial projection using the same pacing point combination demonstrating absence of a target area.

Figures

Figure 1

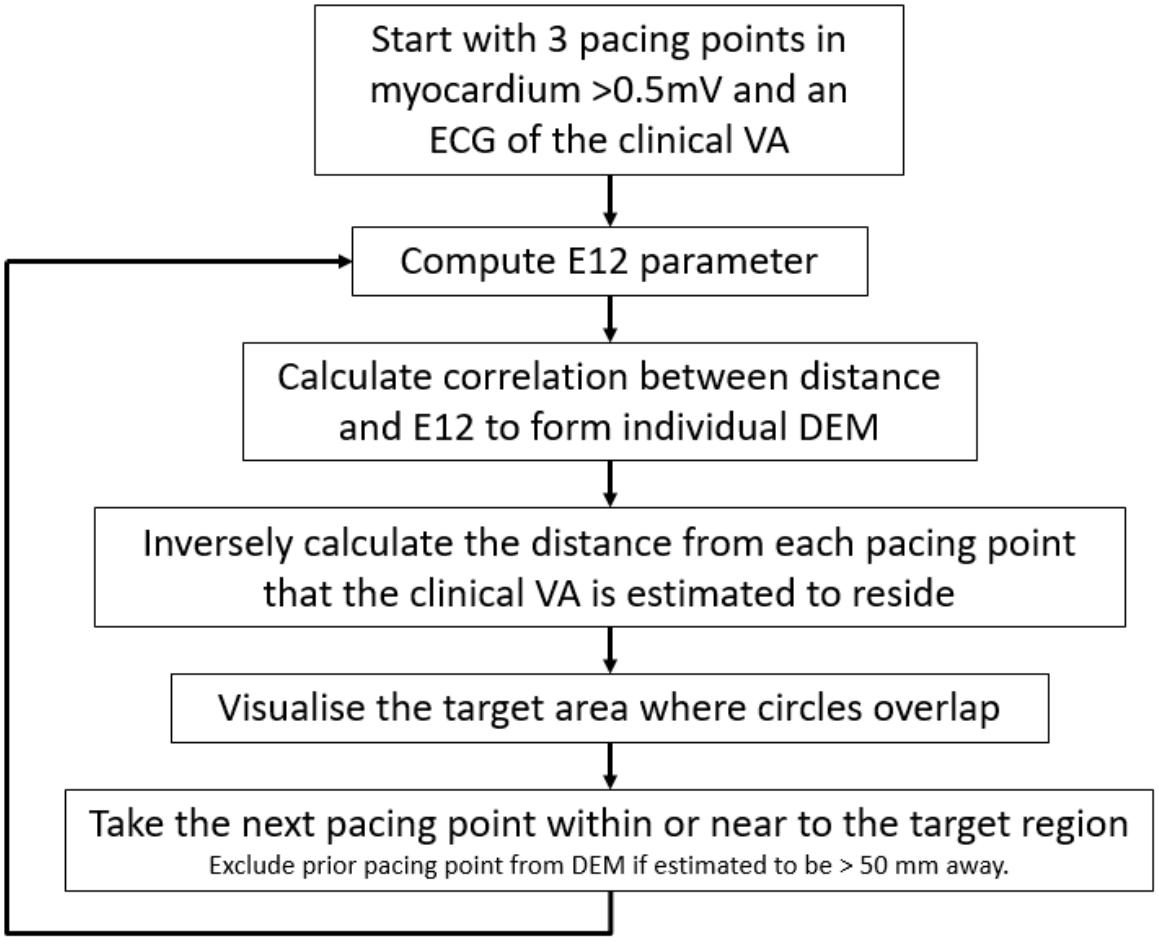

Figure 2

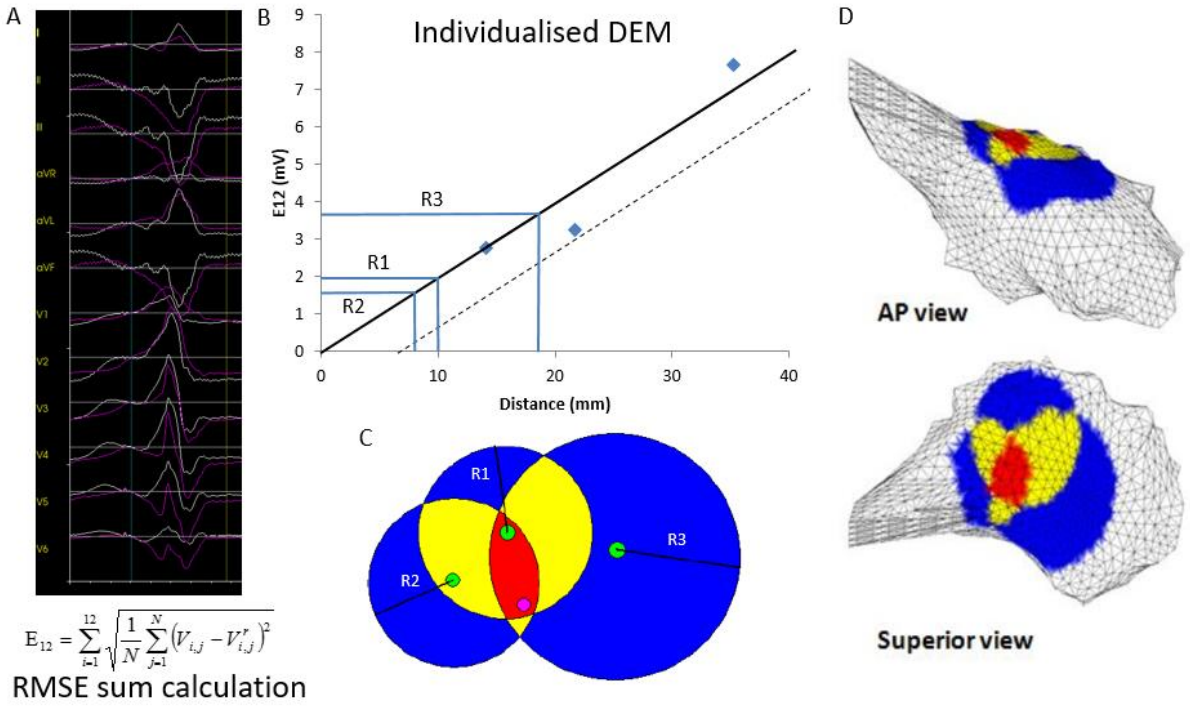
A
B
Individualised DEM
E12 (mV)
Distance (mm)
R1
R2
R3
C
D
AP view
Superior view
RMSE sum calculation

Figure 3

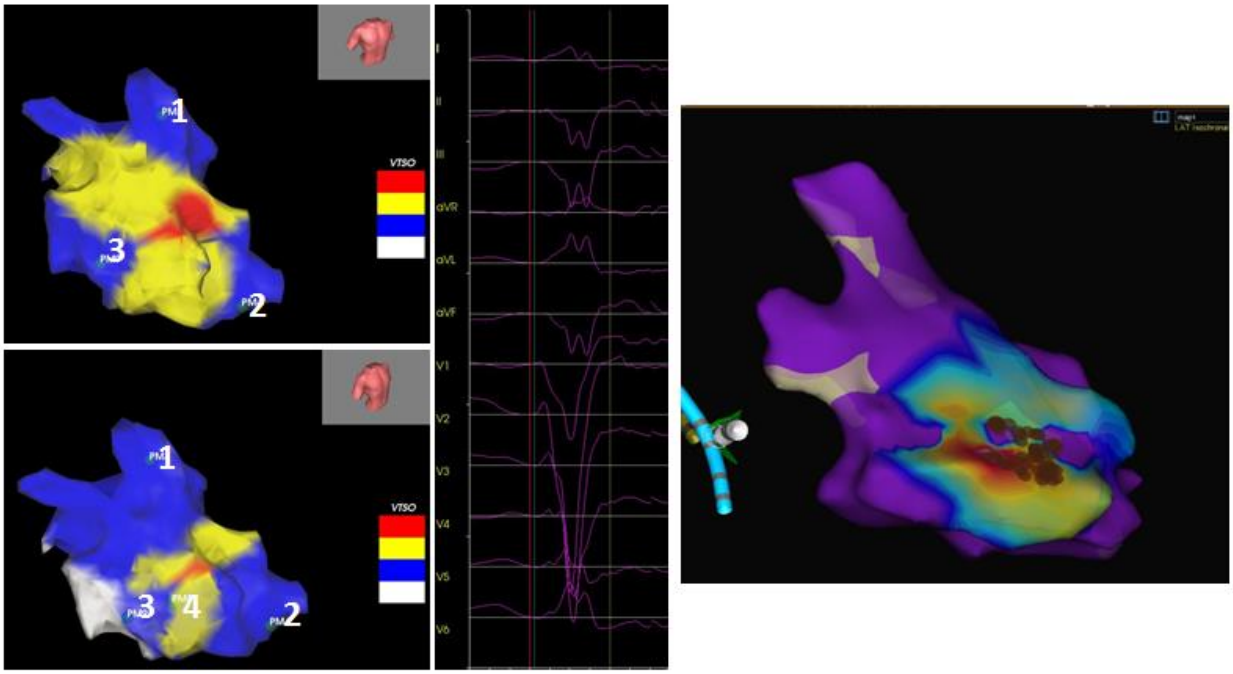
PM1
PM3
PM2
VTSO
I
II
III
aVR
aVL
aVF
V1
V2
V3
V4
V5
V6
PM1
PM3
PM4
PM2
VTSO

Figure 4

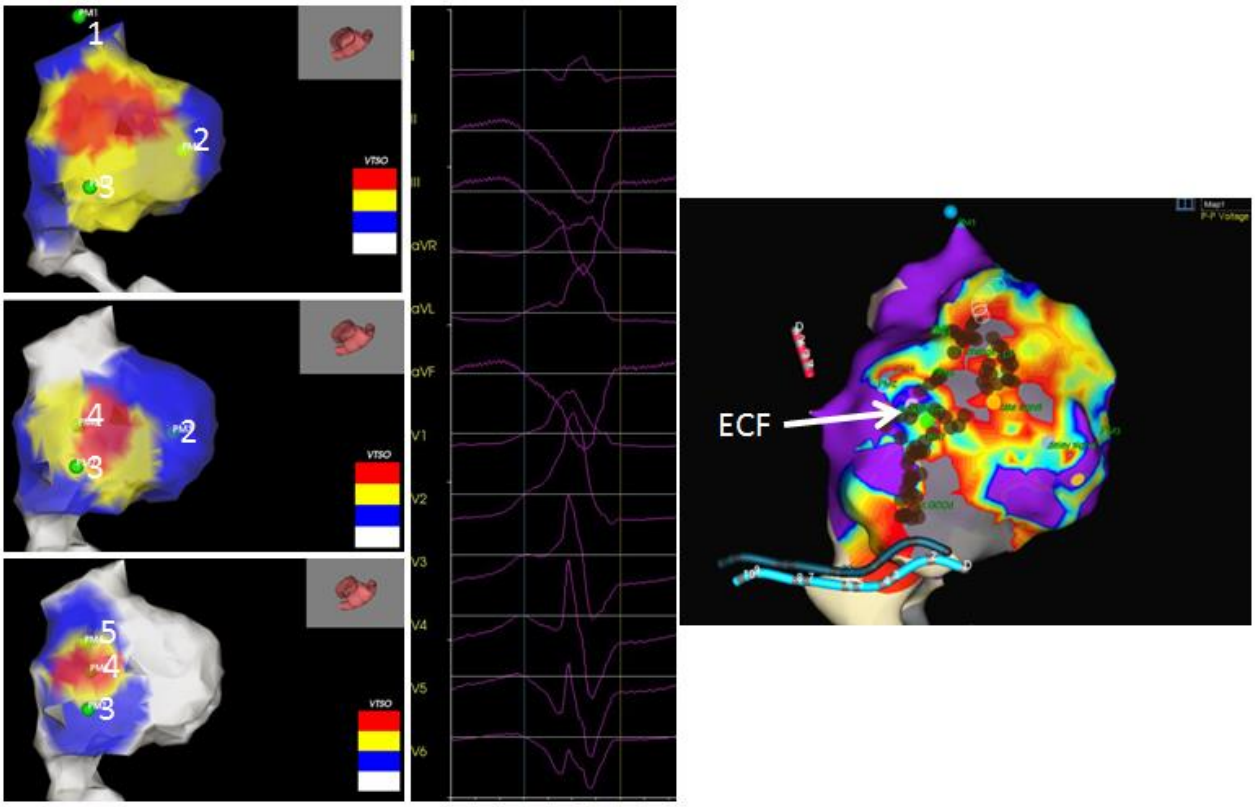
1
2
3
VTSO
4
2
3
VTSO
5
4
3
VTSO
I
II
III
aVR
aVL
aVF
V1
V2
V3
V4
V5
V6
ECF

Figure 5

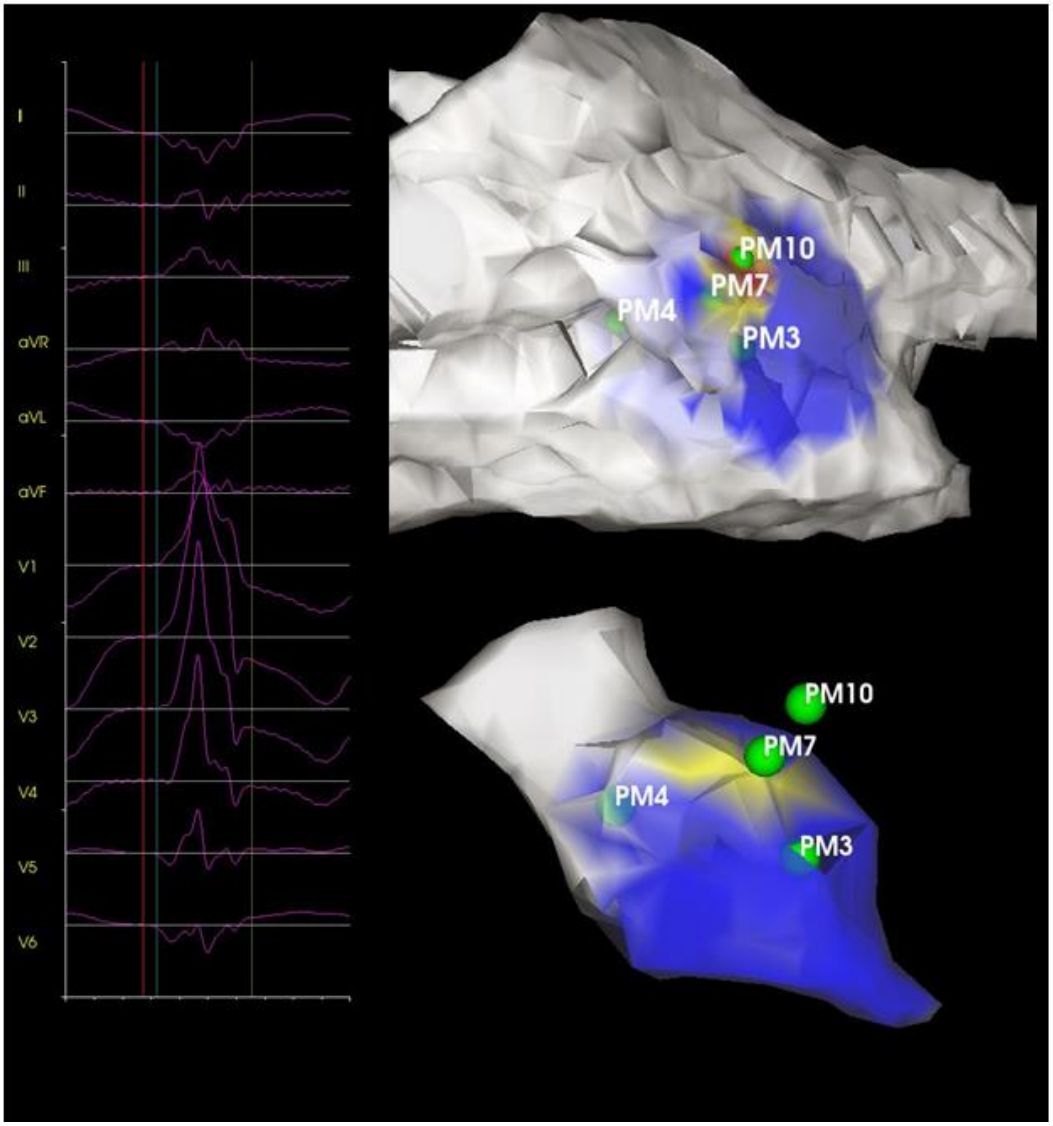
I
II
III
aVR
aVL
aVF
V1
V2
V3
V4
V5
V6
PM10
PM7
PM4
PM3
PM10
PM7
PM4
PM3

Tables

Table 1. Baseline patient demographics

	Normal heart n=16(50%)	**Scar** n=16(50%)	**P value**
Age, mean(SD)	43(12)	63(14)	≤0.001
Gender male, n(%)	6(38)	15(94)	0.001
NYHA class, n(%)			
I	13(92)	4(29)	
II	1(8)	8(57)	
III	0	2(14)	
IV	0	0	
Scar aetiology, n(%)			
Ischemic	0	7(44)	
DCM	0	3(19)	
ARVC	0	2(12)	
Myocarditis	0	3(19)	
CPVT	1	0	
Glycogen storage	0	1(6)	
Baseline Creatinine, g/dL, med(IQR)	74(20)	97(39)	0.004
Ejection fraction, %, med(IQR)	60(8)	45(26)	0.001
Medical history, n(%)			

DM	0	2	0.484
COPD	0	3	0.226
HT	1	4	0.333
CVA	0	1	1
AF	1	4	0.333
CABG	0	4	0.101
PCI	0	1	1
Device, n(%)			
None	0	4(25)	
ICD	1(6)	6(38)	
CRT-D	0	5(31)	
CRT-P	0	1(6)	
ICD indication, n(%)			
Primary prevention	1	5(31)	
Secondary prevention	0	6(37)	
Medication n(%)			
Beta blocker	9(56)	14(88)	0.113
Amiodarone	0	8(50)	0.002
Sotalol	0	0	
Lidocaine	0	1(6)	1
Mexiletine	0	1(6)	1
Verapamil	1(6)	0	1
Flecainide	2(13)	0	0.484
ACEi/ARB	3(19)	13(81)	<0.001
Statin	1(6)	10(62)	0.001

Aldosterone blocker	0	6(38)	0.018
Previous ablations, n	1	5	

Table 2. Procedural characteristics

	Normal heart n=16	**Scar** n=19	**P value**
Procedure type n(%)			
VE	13(81)	6(32)	
VT	3(19)	13(68)	
Indication n(%)			
Symptoms	13(81)	4(21)	
ICD shocks	0	5(26)	
VT storm	1(6)	3(16)	
Presumed VA cardiomyopathy	2(13)	2(11)	
Prevention of shocks	0	4(21)	
Suboptimal CRT pacing	0	1(5)	
Anaesthesia n(%)			
Sedation	12(75)	2(11)	
General	4(25)	17(89)	
Approach, n(%)			
Endocardial	16	16(84)	
Endocardial/Epicardial	0	3(16)	
Procedure length, m, mean(SD)	165(55)	223(88)	0.023
Fluoroscopy time, m, med(IQR)	25(14)	26(25)	0.260
Number of RF applications, mean(SD)	14(8)	18(7)	0.163
RF duration, s, med(IQR)	765(1026)	1763(1244)	0.001
Acute endpoint, n(%)			

Success	10(63)	18(95)	
Partial success	5(31)	1(5)	
Fail	1(6)	0	
Complications, n			
Intraprocedural	0	0	
30 day			
Tamponade	0	1	
Phrenic nerve palsy	0	1	

Table 3. Procedural mapping data

	Normal heart n=16	**Scar** n=19	**P value**
Number of VAs mapped with system	18	28	
Location of VAs mapped, n			
LV LVOT RV RVOT Epicardial LV	2 3 3 10 0	22 2 1 1 2	
Target size mm^2, med(IQR)	208.9(126.6)	187.4(180.3)	0.80
Number of Pacing sites used for DEM, med(IQR)	4(1)	5(2)	0.33
Pacing output mV, med(IQR)	2(3.5)	2.6(2)	0.66
Pacing latency ms, med(IQR)	25(14)	32(15)	<0.001
Correlation values, R^2, med(IQR)	0.963(0.098)	0.945(0.049)	0.74
Variance – Mean square error, mean(SD)	3.92(2.38)	3.67(2.10)	0.87
Slope of DEM, mean(SD)	0.258(0.108)	0.274(0.117)	0.64

DEM = distance-E12 model; VA = ventricular arrhythmia